

Plasma Sci. Technol. **19** (2017) 045401 (6pp) https://doi.org/10.1088/2058-6272/aa57f3

Dynamic behavior of a rotating gliding arc plasma in nitrogen: effects of gas flow rate and operating current

Hao ZHANG (张浩)[1,2,4], **Fengsen ZHU** (朱凤森)[2], **Xiaodong LI** (李晓东)[2] **and Changming DU** (杜长明)[3]

[1] Institute of Energy and Power Engineering, College of Mechanical Engineering, Zhejiang University of Technology, Hangzhou 310014, People's Republic of China
[2] State Key Laboratory of Clean Energy Utilization, Zhejiang University, Hangzhou 310027, People's Republic of China
[3] School of Environmental Science and Engineering, Sun Yat-sen University, Guangzhou 510275, People's Republic of China

E-mail: zhanghao0320@zjut.edu.cn

Received 8 November 2016, revised 7 December 2016
Accepted for publication 16 December 2016
Published 9 March 2017

Abstract

The effects of feed gas flow rate and operating current on the electrical characteristics and dynamic behavior of a rotating gliding arc (RGA) plasma codriven by a magnetic field and tangential flow were investigated. The operating current has been shown to significantly affect the time-resolved voltage waveforms of the discharge, particularly at flow rate $= 2\,\mathrm{l\,min^{-1}}$. When the current was lower than 140 mA, sinusoidal waveforms with regular variation periods of 13.5–17.0 ms can be observed (flow rate $= 2\,\mathrm{l\,min^{-1}}$). The restrike mode characterized by serial sudden drops of voltage appeared under all studied conditions. Increasing the flow rate from 8 to $12\,\mathrm{l\,min^{-1}}$ (at the same current) led to a shift of arc rotation mode which would then result in a significant drop of discharge voltage (around 120–200 V). For a given flow rate, the reduction of current resulted in a nearly linear increase of voltage.

Keywords: rotating gliding arc (RGA), electrical characteristics, gas flow rate, operating current, rotation mode

(Some figures may appear in colour only in the online journal)

1. Introduction

Electrically generated plasmas are generally classified into two major types: thermal and non-thermal, each of which has its advantages and drawbacks [1, 2]. Thermal plasma, which enables the use of high power (e.g., 50 MW) [1, 3], allows for a rapid start-up of some thermodynamically unfavorable processes such as the vitrification of air pollution control residues [4], whereas, due to the equilibrium or quasi-equilibrium state of thermal plasma, it lacks chemical selectivity, which is of primary importance to plasma chemistry [1]. In addition, the high gas temperature in thermal plasma (over 10^4 K) causes serious cooling requirements and electrode erosion problems, which limits its process efficiency and applicability [1, 2]. On the other hand, non-thermal plasma exhibits a relatively low gas temperature (300–1500 K) [5], while the energetic electrons have a high temperature of up to 1–5 eV ($(1–5) \times 10^4$ K), which play a key role in non-thermal plasma chemical reactions. Therefore, the non-thermal plasma is chemically more selective [6, 7]. Nevertheless, the potential large scale application of non-thermal plasma is significantly restricted by its relatively low power level [1, 8]. For plenty of promising plasma chemical applications, an energy-efficient productivity with high power and the nonequilibrium characteristics of non-thermal plasma to provide selective reactions are both required [1].

Gliding arc discharge (GAD)—which typically comprises two divergent electrodes with a knife shape and is shown to be a

[4] Author to whom any correspondence should be addressed.

powerful transitional plasma with a relatively high power, high electron temperature, good selectivity for chemical process, as well as high energy efficiency [1, 8–12]—has been extensively studied and successfully applied in a number of applications over the past decade, such as energy conversion [9, 13–17], CO_2 reduction [18, 19], enhancement of combustion [12, 20], material treatment [21], air sterilization [10, 22], and environmental applications (e.g., destruction of volatile organic compounds (VOC) [23, 24] and waste water disposal [25]).

Although GAD has been shown to be promising for many applications, this technology has several important drawbacks, including: limited plasma reaction volume due to the two-dimensional electrode geometry; the unstable sustaining of plasma parameters that are probably unfavourable for some applications; inhomogeneous treatment of the feed gas due to the nonuniform distribution of arc discharge in the reactor; a low retention time of reactant gases in plasma zone resulting from the high gas flow rate demand (e.g., 10–20 l min^{-1}) [1, 5, 14], which limit the performance and applicability of the processes.

To solve the above problems, a direct current (DC) powered rotating gliding arc (RGA) discharge co-driven by a magnetic field and tangential flow has been developed in our lab [5, 26]. In the RGA reactor, the gliding arc can rotate steadily and rapidly without extinction under the synergetic effects of the Lorentz force and swirling flow (the rotation frequency can reach 120 rotations per second), forming a three-dimensional plasma disc area in which the retention time of a reactant gas can be significantly increased with improved reaction performance. We have shown that the RGA plasma significantly favoured the conversion of methane for H_2 production with a maximum CH_4 conversion rate of 91.8%, a selectivity for H_2 of 80.7%, and a minimum energy consumption for H_2 production of 14.3 kJ l^{-1} [5]. The effects of magnetic flux density and types of carrier gas on the motion behavior, time-resolved electrical signals, and spectroscopic characteristics of the RGA discharge have also been investigated [26, 27]. Nevertheless, further studies on the stability and dynamic behavior of this promising technology are still extremely necessary for a better understanding of its properties and establishing a basis for potential applications.

Feed gas flow rate and operating current have been identified as two key parameters affecting strongly the stability and operation regimes of the arc [28, 29]. In this study, we will investigate the effects of these two parameters on the electrical characteristic, dynamic behavior, and stability of the RGA discharge in N_2.

2. Experiment

The experimental setup is schematically shown in figure 1, which mainly comprises a mass flow controller (MFC), RGA reactor, power supply system, and detecting system. The reactor configuration is given in figure 1 as well. A stainless steel inner electrode (100 mm in height) serves as the anode and a ground stainless steel cylinder (36 mm inner diameter) serves as the cathode. The arc is ignited at the narrowest gap point (2 mm) between the electrodes. Three tangential entrances were located at the bottom for the injection of N_2. In this way, a swirling N_2 gas flow was formed in the reactor. An annular permanent magnet surrounded the cylinder reactor to form an upward magnetic field in the reactor (around 2000 G in flux density). Therefore, a Lorentz force was generated on the arc current, which had a stabilizing and accelerating effect on the rotation of the arc. Finally, the arc rotated steadily and rapidly around the cone-shaped anode under the synergetic effect of swirling flow and Lorentz force, generating a stable plasma 'disc' area.

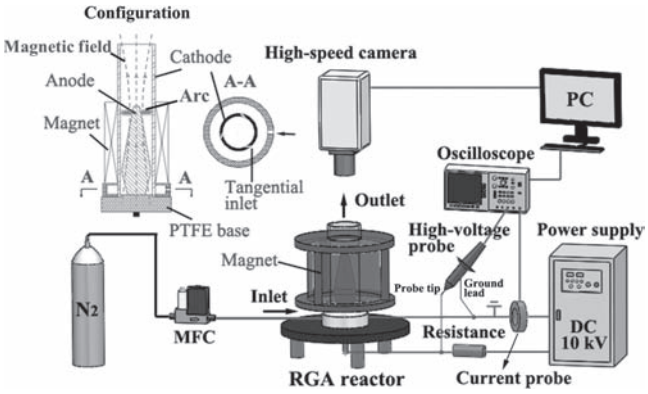

Figure 1. Schematic of the experimental setup.

The feed flow rate Q was adjusted using a MFC (D07-series, Sevenstar). A 10 kV DC power supply was used to generate the RGA plasma, and a resistance of 40 kΩ was connected to the power supply to restrict the discharge current and inhibit over-heating of the plasma. During the experiments, the operating current was adjusted by the power supply while the feed flow rate was fixed at 2, 8, or 12 l min^{-1} to investigate the effects of operating current and feed flow rate.

An oscilloscope (Tektronix DPO4034B, 350 MHz analog bandwidth, 2.5 GS s^{-1} sample rate) equipped with a high-voltage probe (Tektronix P6015A) and a current probe (Tektronix TCP303) was employed to measure the time-resolved voltage and current signals of the discharge. In the measurement, the tip of the high-voltage probe was connected to the inner electrode of the reactor and the ground lead was grounded. The current probe was clamped around the electric wire that connected to the outer electrode of reactor. The discharge power was calculated based on the instantaneous voltage and current obtained by the oscilloscope. A high-speed digital camera (HG-100K) equipped with a CMOS sensor was used to record the motion behavior of the gliding arc. The frame speed and exposure time were set at 1000 frames per second (fps) and 997 μs, respectively.

3. Results and discussion

3.1. Effect of flow rate and operating current on time-resolved voltage waveforms

Figure 2 shows the typical time dependence of the discharge voltage with different operating currents at $Q = 2\,l\,min^{-1}$.

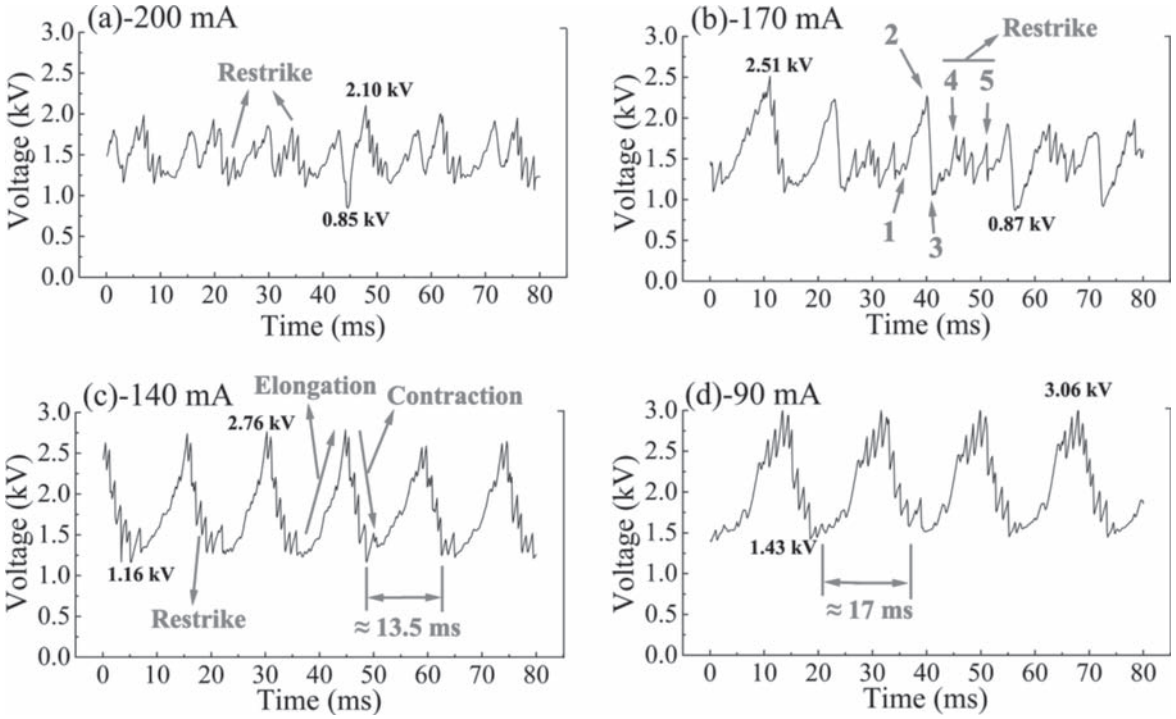

Figure 2. Time-resolved voltage waveforms with different operating currents at $Q = 2\,\mathrm{l\,min^{-1}}$.

Note that the operating current here represents the mean value of the discharge current displayed by the power supply. It can clearly be seen that the operating current I significantly influences the electrical characteristics of the RGA plasmas. Decreasing the current leads to the formation of a more and more regular voltage waveform, which can probably be partially attributed to the increased discharge voltage (see figure 4) that has a stabilizing effect on the discharge. For $I \geqslant 170$ mA (figures 2(a)–(b)), the voltage waveforms show instabilities without regular periods.

It should be noted that, for DC gliding arc discharges with such a low current (<250 mA in this study), the discharge properties have been shown to correspond to a glow-type discharge rather than an arc discharge [30–32].

Our previous study on the motion behavior of the rotating arc has shown that the formed arc column would elongate gradually under the simultaneous force of swirling flow and Lorentz force, and then contract abruptly during the rotation of the arc. This process repeats periodically with a period of around 8–16 ms, which is similar to that of the voltage waveform in figure 2. Therefore, we can infer that in figure 2(b) the nearly linear increase (point 1 to 2, typically a 870–1300 V lift with an increase rate of 241.5–381.7 $\mathrm{kV\,s^{-1}}$) and drastic drop (point 2 to 3, with a decrease rate of around 1.63 $\mathrm{MV\,s^{-1}}$) of the discharge voltage correspond to the gradual elongation and abrupt contraction of the column of the arc respectively along with the motion of arc spots.

Interestingly, from point 4 to 5, a small sawtooth waveform characterized by a slow rise of voltage followed by a sudden drop of voltage (typically a 180–450 V drop with a decrease rate of 2.6–3.4 $\mathrm{MV\,s^{-1}}$) can also be observed. The sawtooth waveform is quite similar to that from point 1 to 3, but has a much smaller fluctuation amplitude and shorter period.

As denoted in figure 2(b), the restrike mode of waveform, which has been extensively reported in DC plasma torches [33, 34] and is characterized by small sawtooth electrical signals, can be observed. As explained in our previous work [27], the restrike mode is considered to be caused by the presence of a gas boundary layer with steep gradients that formed at the arc spots on the cathode [35–37]. Tu *et al* have also found the restrike mode of waveform in traditional flat GAD reactors [35, 38]. Figure 2(a) with $I = 200$ mA shows a waveform similar to figure 2(b), only with a lower fluctuation amplitude.

When the operating current decreases to 140 mA, the waveform shows a nearly sinusoidal shape with a regular variation period of around 13.5 ms. The discharge voltage rises and declines repeatedly (a peak-to-peak amplitude of typically 1320–1620 V with a growth rate of 140–200 $\mathrm{kV\,s^{-1}}$ and a decline rate of 350–415 $\mathrm{kV\,s^{-1}}$). One possible explanation for the occurrence of the regular waveform is that decreasing the arc current could result in a drop in both the electron density and gas temperature, and so the density and temperature gradients between the arc and electrode wall will also decrease [39]. As a consequence, the drag force that the arc root experiences from the electrode might decrease, resulting in the occurrence of a regular and smooth motion of the arc spots. The discharge voltage varies proportionally with the length of the arc column. It should be noted that the restrike modes can also be observed along with the rise and fall of the discharge voltage, as can be seen in figure 2(c), indicating the occurrence of breakdown in the gas boundary layer during

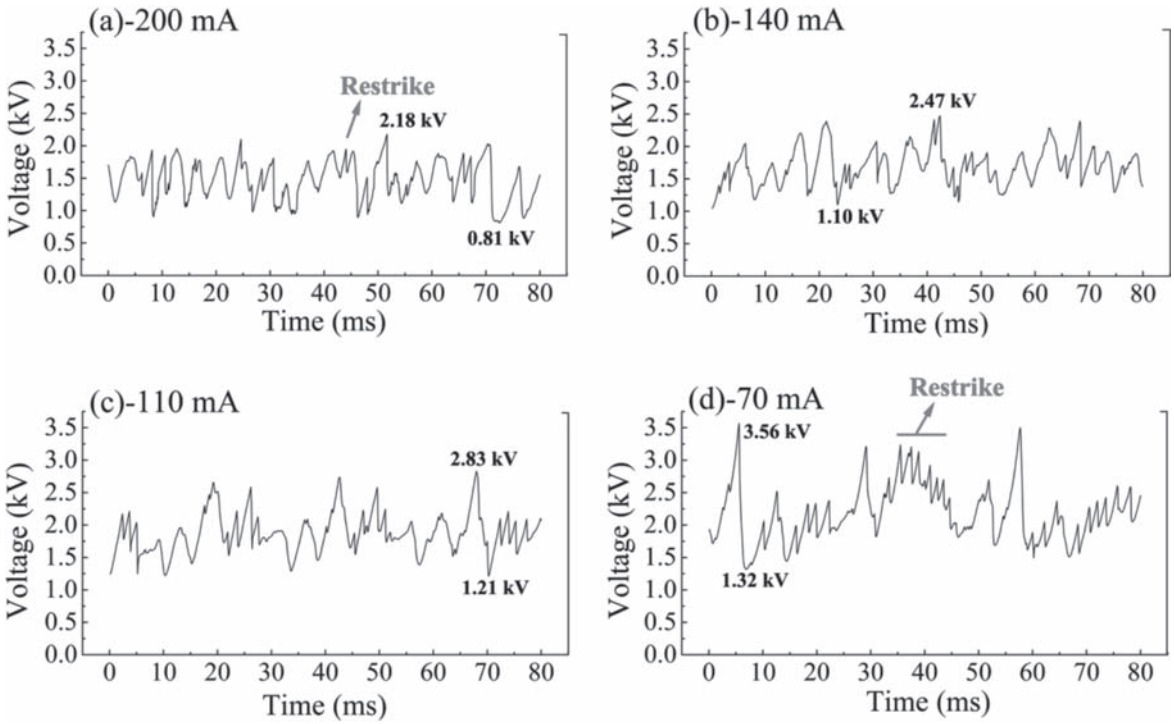

Figure 3. Time-resolved voltage waveforms with different operating currents at $Q = 8\,\mathrm{l\,min^{-1}}$.

the smooth rotation of the arc in this case. For $I = 90$ mA in figure 2(d), we can also see a similar waveform with a more or less sinusoidal shape. With the decrease of operating current, the variation period of the voltage tends to increase, for instance, from $I = 140$ to 90 mA, the period rises from 13.5 to 17.0 ms, which should arise from the decreased rotation frequency of the arc due to the drop in current. Our previous study has shown that the rotation frequency of the arc is positively correlated with the discharge current because the arc experiences a Lorentz force from the magnetic field [26]. It is also interesting to note that the restrike mode tends to appear more frequently at a lower operating current (e.g., 90 mA (figure 2(d))), which might be ascribed to the increased discharge voltage (i.e., electric field intensity) that could result in a more frequent breakdown through the boundary layer, as can be seen from figure 2.

Typical voltage waveforms of the RGA discharge with different operating currents at $Q = 8\,\mathrm{l\,min^{-1}}$ are shown in figure 3. We can see that, compared to figure 2, the voltage waveforms at $Q = 8\,\mathrm{l\,min^{-1}}$ appear to be more irregular without sinusoidal waveforms for all tested currents. This might be attributed to the increased arc fluctuation that resulted from the increase in the turbulent intensity of the gas flow. In addition, it is found that a decrease of current from 200 to 70 mA seems to lead to an increase in the peak-to-peak amplitudes of voltage from 470–1220 V to 850–2250 V. Similar behavior was also observed in DC plasma torches [39, 40].

For a higher flow rate ($Q > 8\,\mathrm{l\,min^{-1}}$), the voltage waveforms at different operating currents were similar to that in figure 3 ($Q = 8\,\mathrm{l\,min^{-1}}$).

3.2. Effect of flow rate and operating current on discharge voltage and power

The variations of the mean discharge voltage and discharge power with decreasing operating current at different flow rates (2, 8, and $12\,\mathrm{l\,min^{-1}}$) are shown in figure 4. The discharge power P was calculated using the following formula:

$$P(W) = (1/T)\int_0^T u(t)\cdot i(t)\mathrm{d}t = \sum_{j=1}^{N} u_j i_j / N \qquad (1)$$

where T means the total time of a selected cycle; $u(t)$, $i(t)$ represent the instantaneous voltage and current at time t respectively; and N indicates the number of records.

During the experiment, the flow rate was fixed and the operating current was progressively decreased until an instable operation of the arc was observed, when the discharge could not be stabilized as a rotating plasma disc but started an evolution of ignition, elongation, extinguishment, and reignition. We can see from figure 4(a) that, at a fixed flow rate, the mean voltage rises nearly linearly with decreasing current, resulting from the increase of electrical resistance as the current intensity declines [35, 41, 42]. Similar dropping curves have been reported in normal glow discharges [41, 43], alternating current (AC) RGA discharges [44], and DC plasma torches [42].

At a fixed operating current, an increase of gas flow rate from 2 to $8\,\mathrm{l\,min^{-1}}$ leads to an increase in voltage. This should be attributed to the increased heat loss and the need to sustain the arc discharge by increasing the voltage [39]. However, with a further increase of flow rate to $12\,\mathrm{l\,min^{-1}}$ (at the same current), a significant drop of voltage (around

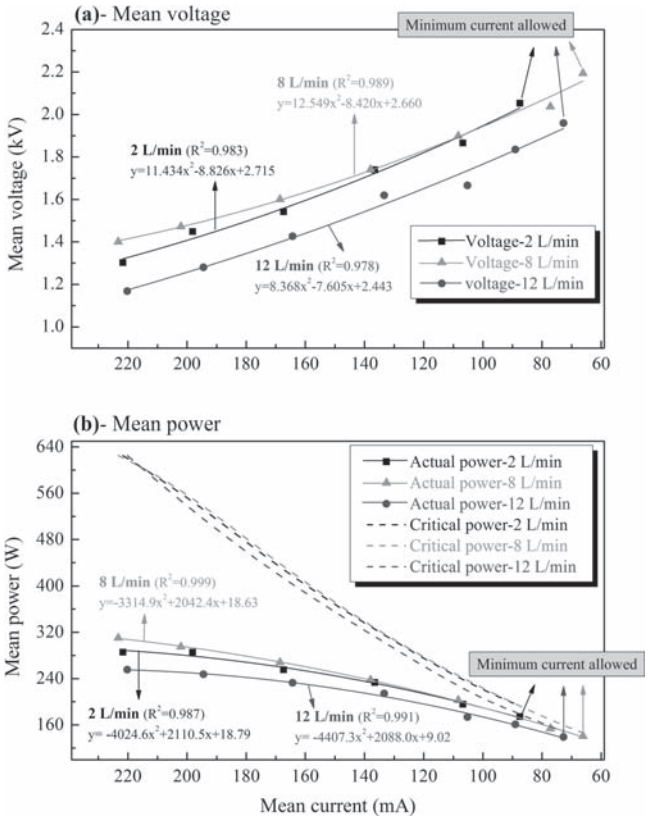

Figure 4. Variations of the mean discharge voltage (a) and power (b) with decreasing operating current at different flow rates (2, 8, and 12 l min^{-1}). Solid lines are polynomial fits to the data points.

120–200 V) occurs, as shown in figure 4(a), which should be caused by the shift of arc position.

Two modes of arc rotation can be observed depending on the feed flow rates in the RGA reactor, as shown in figure 5. The increase of flow rate from 8 to 12 l min^{-1} resulted in a shift of the rotating arc from position A to B, which was responsible for the drop on voltage (figure 4(a)) due to the remarkable decrease of the arc length [26, 29]. An explanation for this phenomenon is available in our previous work [27].

Interestingly, Lee *et al* also reported the presence of three motion modes of a rotating arc, exhibiting different motion behaviors and arc lengths in an AC RGA plasma driven by tangential flow, depending on the input energy density [29]. The arc length has been considered as a critical parameter for the plasma-reforming process. A longer arc length can lead to an increase in the non-equilibrium characteristics of the plasma as well as a larger effective plasma reaction zone and has been proved to significantly enhance the plasma chemistry [29, 45, 46]. In this study, a gas flow rate of lower than 12 l min^{-1} is recommended because a longer arc length and an enhanced retention time of reactants can be obtained simultaneously in this case. It is important to note that, in traditional flat GAD reactors, a high gas flow rate (e.g. 10–20 l min^{-1}) is typically needed for the sustaining of arc discharge, which will in turn lead to a drop in the reactor efficiency because of the decreased residence time of reactants in the plasma area [47–49].

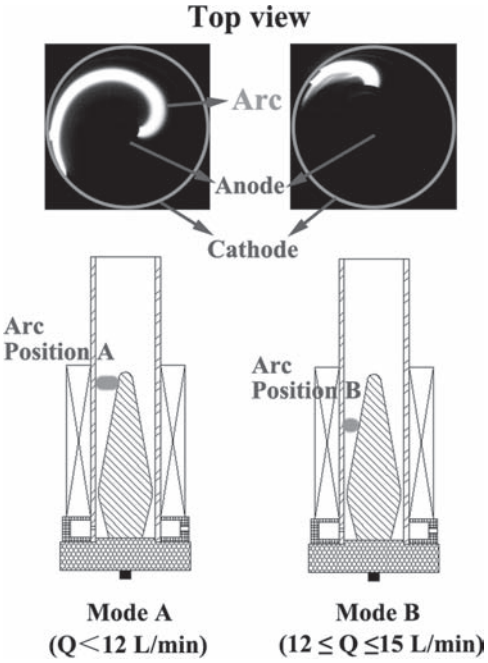

Figure 5. Schematics of the two rotation modes of the arc.

As shown in figure 4(b), for a given operating current, the increase of voltage leads to a lift in the discharge power, whereas at a fixed flow rate, the discharge power follows an opposite trend with the voltage as the operating current reduces.

For a given DC circuit, an Ohm law relationship for the total applied voltage (U_p) can be written as [2]

$$U_p = R \cdot I + U = R \cdot I + P/I \tag{2}$$

where R is the external resistance (40 kΩ), U is the discharge voltage, and I is the current.

The solutions for I can be obtained as

$$I = (U_p \pm \sqrt{U_p^2 - 4PR})/(2R). \tag{3}$$

To obtain a positive value of I, the discharge power should satisfy the condition

$$P \leqslant U_p^2/(4R). \tag{4}$$

Therefore, the actual discharge power must be lower than this critical power ($U_p^2/(4R)$) to achieve a stable operation of the discharge (the arc rotates rapidly and steadily on a plane). If the actual discharge power exceeds the critical power, an instable operation of the arc will occur (as described previously). The value of the critical power ($U_p^2/(4R)$) for each flow rate as a function of current has been illustrated in figure 4(b). It can clearly be seen that the actual minimum power allowed reaches exactly at the intersection of the actual power line and the calculated critical power line, confirming the validity of the above analysis.

4. Conclusion

The electrical characteristics and dynamic behavior of the RGA plasma have been shown to be strongly dependent on the feed gas flow rate and operating current. At a flow rate $= 2\,\mathrm{l\,min^{-1}}$, for an operating current of lower than 140 mA, the voltage waveforms exhibited a more or less sinusoidal waveform with a regular variation period of 13.5–17.0 ms. The restrike mode characterized by several serial sudden drops of voltage appeared under all studied conditions.

Two modes of the arc rotation can be observed depending on the feed flow rate in the RGA reactor, exhibiting different motion behavior and lengths of arc discharge. The shift of arc rotation mode from a higher position to a lower position led to a significant drop of discharge voltage (around 120–200 V) as the flow rate increased from 8 to $12\,\mathrm{l\,min^{-1}}$ (at the same current). For a given flow rate, the reduction of current led to a nearly linear increase of voltage.

For a given operating current, the increase of voltage led to an increase in the discharge power, whereas at a fixed flow rate, the discharge power followed an opposite trend with the voltage as the operating current reduced. The actual discharge power must be lower than a critical power of $U_p^2/(4R)$ (U_p is the total applied voltage, R is the external resistance) to achieve a stable operation of the discharge (the arc rotates rapidly and steadily on a plane).

Acknowledgments

This work is supported by National Natural Science Foundation of China (51576174).

References

[1] Kalra C S *et al* 2005 *Rev. Sci. Instrum.* **76** 025110
[2] Fridman A *et al* 1999 *Prog. Energy Combust. Sci.* **25** 211
[3] Tu X *et al* 2007 *J. Phys. D: Appl. Phys.* **40** 3972
[4] Tu X *et al* 2010 *IEEE Trans. Plasma Sci.* **38** 3319
[5] Zhang H *et al* 2014 *Int. J. Hydrogen Energ.* **39** 12620
[6] Liu S Y *et al* 2014 *J. Phys. Chem.* C **118** 10686
[7] Mei D H *et al* 2015 *Plasma Sources Sci. Technol.* **24** 015011
[8] Kalra C S, Gutsol A F and Fridman A A 2005 *IEEE Trans. Plasma Sci.* **33** 32
[9] Tu X and Whitehead J C 2014 *Int. J. Hydrogen Energ.* **39** 9658
[10] Du C M *et al* 2014 *IEEE Trans. Plasma Sci.* **42** 2221
[11] Mitsugi F *et al* 2014 *IEEE Trans. Plasma Sci.* **42** 3681
[12] Bublievsky A F *et al* 2015 *IEEE Trans. Plasma Sci.* **43** 1742
[13] Gutsol A, Rabinovich A and Fridman A 2011 *J. Phys. D: Appl. Phys.* **44** 274001
[14] Li X D *et al* 2013 *IEEE Trans. Plasma Sci.* **41** 126
[15] Zhang H *et al* 2016 *RSC Adv.* **6** 12770
[16] Zhang H *et al* 2015 *Int. J. Hydrogen Energ.* **40** 15901
[17] Zhang H *et al* 2016 *Plasma Chem. Plasma Process.* **36** 813
[18] Wang W Z and Bogaerts A 2016 *Plasma Sources Sci. Technol.* **25** 055025
[19] Wang W Z *et al* 2016 *Plasma Sources Sci. Technol.* **25** 065012
[20] Ombrello T, Ju Y and Fridman A 2008 *AIAA J.* **46** 2424
[21] Kusano Y *et al* 2013 *J. Phys. D: Appl. Phys.* **46** 135203
[22] Cooper M *et al* 2008 Sterilization and complete removal of bacteria using atmospheric pressure plasmas *Proc. of the 35th IEEE Int. Conf. on Plasma Science (Karlsruhe, Germany)* (https://doi.org/10.1109/PLASMA.2008.4591007)
[23] Yu L *et al* 2010 *J. Hazard. Mater.* **180** 449
[24] Zhu F S *et al* 2016 *Fuel* **176** 78
[25] Ni M J *et al* 2015 *Plasma Sci. Technol.* **17** 209
[26] Zhang H *et al* 2012 *IEEE Trans. Plasma Sci.* **40** 3493
[27] Zhang H *et al* 2016 *Plasma Sci. Technol.* **18** 473
[28] Mutaf-Yardimci O *et al* 1999 *Ann. NY Acad. Sci.* **891** 304
[29] Lee D H *et al* 2007 *Proc. Combust. Inst.* **31** 3343
[30] Korolev Y D *et al* 2011 *IEEE Trans. Plasma Sci.* **39** 3319
[31] Korolev Y D *et al* 2014 *Plasma Sources Sci. Technol.* **23** 054016
[32] Korolev Y D *et al* 2014 *IEEE Trans. Plasma Sci.* **42** 1615
[33] Dorier J L *et al* 2001 *IEEE Trans. Plasma Sci.* **29** 494
[34] Duan Z and Heberlein J 2002 *J. Therm. Spray Technol.* **11** 44
[35] Tu X *et al* 2009 *Phys. Plasmas* **16** 113506
[36] Tu X *et al* 2008 *Phys. Plasmas* **15** 053504
[37] Eckert E R G, Pfender E and Wutzke S A 1967 *AIAA J.* **5** 707
[38] Tu X, Gallon H J and Whitehead J C 2011 *IEEE Trans. Plasma Sci.* **39** 2900
[39] Tu X *et al* 2007 *Plasma Sources Sci. Technol.* **16** 803
[40] Kaminska A and Dudeck M A 1998 *High Temp. Mater. Process. (NY)* **2** 117
[41] Staack D *et al* 2005 *Plasma Sources Sci. Technol.* **14** 700
[42] Ma J *et al* 2015 *Chin. Phys.* B **24** 065205
[43] Staack D *et al* 2006 *Plasma Sources Sci. Technol.* **15** 818
[44] Wu W W *et al* 2015 *IEEE Trans. Plasma Sci.* **43** 3979
[45] Lee D H *et al* 2010 *Int. J. Hydrogen Energ.* **35** 4668
[46] Lee D H *et al* 2010 *Int. J. Hydrogen Energ.* **35** 10967
[47] Zhu J J *et al* 2015 *Appl. Phys. Lett.* **106** 044101
[48] Zhu J J *et al* 2014 *Appl. Phys. Lett.* **105** 234102
[49] Zhang C *et al* 2012 *IEEE Trans. Plasma Sci.* **40** 2843